PROCEEDINGS OF
THE ROYAL SOCIETY B
BIOLOGICAL SCIENCES

# Decoding the dynamics of dental distributions: insights from shark demography and dispersal

| | |
|---|---|
| Journal: | *Proceedings B* |
| Manuscript ID | Draft |
| Article Type: | Research |
| Date Submitted by the Author: | n/a |
| Complete List of Authors: | Kim, Sora; University of California Merced, Life and Environmental Scienecs; University of Chicago Division of the Physical Sciences, Department of Geophysical Sciences<br>Balk, Meghan ; National Ecological Observatory Network, Paleobiology<br>Eberle, Jaelyn; University of Colorado, Geological Sciences and Museum of Natural History<br>Zeichner, Sarah; University of Chicago Division of the Physical Sciences, Department of Geophysical Sciences; California Institute of Technology, Division of Geological and Planetary Sciences<br>Fieman, Dina; Victoria University of Wellington, School of Geography, Environment, and Earth Sciences; University of Colorado Boulder, Department of Geological Sciences<br>Kriwet, Jürgen; University of Vienna, Geozentrum, Palaeontology<br>Yeakel, Justin; University of California Merced, Life and Environmental Sciences |
| Subject: | Ecology < BIOLOGY, Palaeontology < BIOLOGY, Theoretical biology < BIOLOGY |
| Keywords: | sand tiger, body size, latitudinal gradient, Eocene, Arctic, Antarctic |
| Proceedings B category: | Palaeobiology |
| | |

## Author-supplied statements

Relevant information will appear here if provided.

### *Ethics*

*Does your article include research that required ethical approval or permits?:*
This article does not present research with ethical considerations

*Statement (if applicable):*
CUST_IF_YES_ETHICS :No data available.

### *Data*

*It is a condition of publication that data, code and materials supporting your paper are made publicly available. Does your paper present new data?:*
Yes

*Statement (if applicable):*
Raw data for empirical tooth distributions are provided in the Dryad repository XXX.

Simulation code is available in the public GitHub repository
https://github.com/jdyeakel/sharks_bodysize

### *Conflict of interest*

I/We declare we have no competing interests

*Statement (if applicable):*
CUST_STATE_CONFLICT :No data available.

ROYAL SOCIETY OPEN SCIENCE

rsos.royalsocietypublishing.org

Research

Article submitted to journal

**Subject Areas:**
paleontology, ecology, body size, migration, nursery

**Keywords:**
sand tiger, metapopulation, Eocene, Gulf of Mexico, Arctic, Antarctic, Delaware Bay, latitudinal gradient, body size

**Author for correspondence:**
Sora Kim
e-mail: skim380@ucmerced.edu

# Decoding the dynamics of dental distributions: insights from shark demography and dispersal

Sora L. Kim[1,2,*], Justin D. Yeakel[1,*], Meghan Balk[3], Jaelyn J. Eberle[4], Sarah Zeichner[2,5], Dina Fieman[6], Jürgen Kriwet[7]

[1]School of Natural Science, University of California Merced,[2]Department of Geophysical Sciences, University of Chicago, [3]National Ecological Observatory Network, [4]Department of Geological Sciences and Museum of Natural History, University of Colorado, [5]Division of Geological and Planetary Sciences, California Institute of Technology, [6]School of Geography, Environment, and Earth Sciences, Victoria University of Wellington, [7]Department of Paleontology, University of Vienna *Contributed equally

Shark teeth are the most abundant vertebrate fossil, and because tooth size generally correlates with body size, their accumulations document the size structure of populations. Understanding how ecological and environmental processes influence size structure, and how this extends to influence these dental distributions, may offer a window into the ecological and environmental dynamics of past and present shark populations. Here we examine the dental distributions of sand tigers, including extant *Carcharias taurus* and extinct *Striatolamia macrota*, to reconstruct the size structure for a contemporary locality and four Eocene localities. We compare empirical distributions against expectations from a population simulation to gain insight into potential governing ecological processes. Specifically, we investigate the influence of dispersal flexibility to and from protected nurseries. We show that changing the flexibility of initial dispersal of juveniles from the nursery and annual migration of adults to the nursery explains a large amount of dental distribution variability. Our framework predicts dispersal strategies of an extant sand tiger population, and supports nurseries as important components of sand tiger life history in both extant and Eocene populations. These results suggest nursery protection may be vital for shark conservation with increasing anthropogenic impacts and climate change.



THE ROYAL SOCIETY PUBLISHING

## 1. Introduction

Sharks have been a cornerstone of oceanic communities for hundreds of millions of years, a rare constant in a sea of change. The enormous spatial and temporal dominance of shark species suggests considerable ecological plasticity, which has likely contributed to their evolutionary success and may be key to understanding the ongoing and future effects of climate change on this diverse group. Documenting the success of sharks as marine predators has followed a trail of fossilized teeth, accumulating in ocean sediments and indirectly recording their ecological variability as well as the oceanic conditions in which they lived. While shark teeth are the most abundant vertebrate fossil, with a record spanning over 400 million years, the dynamics giving rise to these dental distributions – in particular the interacting effects of shark ecology and the environment – are not well understood.

The geologic record is prolific with fossil shark teeth as well as dermal denticles, both of which document past shark populations and community by way of accumulation. Collections of this material are well-suited to provide insight into the biological organization of shark communities across large spatial and temporal scales. For example, collections of dermal denticles have provided insight into how shark community composition responded to the Cretaceous-Paleogene mass extinction [1], and revealed a severe loss of shark diversity or range shift during the early Miocene [2–4]. It is possible that accumulations of shark teeth within narrow temporal windows can provide insights to the functioning of shark populations and communities because tooth size scales allometrically with body size [5–7]. While fossil shark teeth assemblages have been used to elucidate water temperature and salinity [8,9] as well as species' age distributions [10], ontogenetic stages [11], and the presence of nurseries [12–14], the ecological mechanisms driving population size structure remain enigmatic even in extant populations.

Body size has an enormous influence on the structure and functioning of marine communities [15]. Sharks are gape-limited predators, and gape size scales with body size. Following birth, individuals must acquire enough energy to both build and maintain somatic tissue, achieving reproductive maturity and eventually reaching an asymptotic body size [16]. Because the majority of shark species are ectothermic, the rate at which individuals grow is constrained not only by resource availability [17], but also by water temperature [18]. As temperature varies seasonally and spatially, shark species that migrate between regions are subject to changing growth rates as they transition from juvenile to adult size classes [19,20], and some species may integrate behaviors that take advantage of differentials in resources and temperature to escape smaller body sizes more quickly. For example, many contemporary shark species give birth in warmer estuarine environments where resources are plentiful and large predators are rare, whereupon individuals migrate to colder pelagic environments as they grow [21]. Such life history processes, especially those contributing to dispersal over time and space, will affect their imprint on the dental distributions left behind, and may be one of the few windows into the ecologies of ancient shark species, as well as their relationships to past climates.

The Eocene (56-33.9 Ma) is known for its abundant shark fossil record, with archived collections spanning locations that range from the equator to both poles. This time period may represent a deep-time analogue for the current climate crisis [22], perhaps facilitating a better understanding of how contemporary shark species might respond to similar environmental pressures. Sand tigers occupied a nearly continuous latitudinal gradient ranging from the Arctic to Southern Ocean in the Eocene, demonstrating their remarkable plasticity. The sole evidence of their vast geographical distribution and evolutionary success is contained within local collections of fossilized teeth. For example, high-latitude sites such as Banks Island were deltaic, brackish zones in the Canadian Arctic with reduced salinity [8,23] and low shark diversity [24,25](figure 1, dark green), whereas sites such as Seymour Island off the Antarctic Peninsula were fully marine habitats [26] with high shark diversity [27–31] (figure 1, dark blue). Despite these environmental differences, sand tigers ($^{\dagger}$*Striatolamia macrota*, Agassiz, 1843 and $^{\dagger}$*Carcharias macrota*; extinct species denoted with $^{\dagger}$) occupied both locales during the Eocene [28–33], in addition to lower

latitude environments, notably in the Gulf of Mexico [34](figure 1, lighter shades). Low latitude Eocene sites exhibit an environmental gradient similar to that of the high latitude sites, but in warmer waters with less seasonal variability. For example, the low latitude Red Hot Truck Stop locality of the Tuscahoma and Bashi formations (Fm) in Mississippi was a reduced salinity habitat [35,36] (figure 1, light green), similar to that of Banks Island in the Arctic, whereas the Whiskey Bridge locality of the Crockett Fm. in Texas reflected a more diverse assemblage characteristic of pelagic communities [34,37,38](figure 1, light blue), bearing greater similarity with Seymour Island in the Southern Ocean (figure 1). Compellingly, these dental distributions reveal unique and idiosyncratic attributes, which may encode important ecological relationships governing Eocene sand tiger populations.

Here we examine sand tiger dental distributions from these four Eocene localities that span high- and low-latitudes, as well as a contemporary sand tiger population near Delaware Bay (figure 1). We observe that shark dental distributions vary not only in terms of means and variance, but that some reveal pronounced bimodality while others do not. Given that tooth size and body size are strongly correlated [5–7], such variation in the shapes of local dental distributions may reflect an intersection of environmental and ecological drivers contributing to the presence of different shark size classes in each locality. For example, many shark species migrate to coastal nurseries to reproduce [39,40] and the increased concentration of juveniles at these sites may skew dental distributions to smaller sizes compared to sites in pelagic environments with a higher proportion of adults.

We next assess how temperature, seasonality, and dispersal to and from a nursery, or juvenile, site can affect the shapes of dental distributions. To investigate these effects, we constructed a mechanistic model of a two-site shark metapopulation, where one site serves as a coastal nursery (the juvenile site) and the other serves as a pelagic adult habitat (the adult site) (figure 2). Our population-level framework incorporates temperature-dependent growth, size-dependent first dispersal of juveniles from the nursery to the adult site, and the seasonal dispersal of adults from the pelagic adult site to the coastal nursery. Comparing observed dental distributions to those generated by our model enables a disentangling of likely ecological and environmental mechanisms contributing to observed differences in dental distribution geometries.

Our results point to three key findings. First, we show that changing the flexibility of initial juvenile dispersal to the adult site and annual adult dispersal to the juvenile site have a large effect on dental distribution shape, impacting the mean, variance, and presence or absence of bimodality, all of which feature into shaping empirical distributions. Second, we leverage our framework to correctly predict whether a contemporary sand tiger size structure represents either a juvenile or adult locality, as well as aspects of known life history traits characterizing the dispersal habits of sand tigers occupying the Delaware Bay. Third, we show that our framework, when applied to both contemporary and Eocene sand tiger populations, emphasizes the importance of seasonal adult dispersal as well as the role of juvenile sites serving as nursery localities from the Eocene to the present in both high- and low-latitude localities. That our results support the presence of shark nurseries across a range of oceanic conditions spanning 50 million years lends particular credence to the notion that protecting nursery sites may be vital for shark conservation in the face of future climate change.

## 2. Methods

### (a) Tooth Identification and Measurement

Shark species in the fossil record are largely identified by their tooth morphology [41] due to the poor preservation of cartilaginous skeletons. †*Striatolamia macrota* teeth are identified by emphasized striations on the lingual side relative to the smooth labial side [41]. Anterior teeth (A1-2 and a1-2) are recognized by their long and narrow shape, compared to the lateral and posterior teeth that have a short, blade-like appearance [42]. The anterior teeth have an acute angle between the two roots and have two small lateral cusplets [32,41]. This tooth position was chosen

as a proxy for body size because its large size and distinct morphology compared to other tooth positions within the jaw. Limiting the positions measured from fossil teeth prevents potential for over representation of a single individual within the assemblage. We measured anterior tooth height from the enameloid base to the blade tip with digital calipers to an accuracy of 0.1 mm. The labial and lingual sides of the tooth, and the maximum width was also measured and recorded. The labial side of the tooth is adjacent to the cheek of the shark, and the lingual is that side adjacent to the tongue [41]. Every seventh tooth was re-measured for 0.3 mm accuracy.

The modern analogue for the Eocene †*S. macrota* is the extant sand tiger *C. taurus* based on the similarities in tooth shape throughout the entire dentition [42]. We transformed total length measurements from the 2012 tagging season in Delaware Bay [43–46] to anterior tooth crown height based on the allometric relationships from Shimada et al. [5] and previously applied to fossil *S. macrota* in Kim et al. [10].

For each assemblage, we tested the sample size needed to estimate the mean and standard deviation of the tooth distribution. We then calculated the means and standard deviations of each tooth distribution and performed a power test to calculate the sample size required to estimate the mean and standard deviation within a 95% confidence level and 10% margin of error.

†*Striatolamia macrota* teeth from Banks Island are curated at the Canadian Museum of Nature (Ottawa, ON Canada); Seymour Island are curated at the University of California Museum of Paleontology (UCMP; Berkeley, CA USA), Paleontological Research Institute (PRI; Ithaca, NY USA), and Swedish Natural History Museum (NRM; Stockholm, Sweden); Red Hot Truck Stop locality are curated at the Carnegie Museum of Natural History (CM; Pittsburgh, PA); and Whiskey Bridge locality are curated at the Whiteside Museum of Natural History (WMNH; Seymour, TX). Locality descriptions are included in the Supplementary Materials.

## (b) Population simulation

To explore specific ecological mechanisms that may be responsible for the observed dental distributions, we employed a process-based model allowing us to incorporate likely physiological and ecological constraints influencing shark populations. We constructed a two-site size-class model that tracks female shark populations over time, where one of the two sites is designated a juvenile site, or nursery, and the other is designated an adult site (figure 2). Because there is dispersal from the juvenile to adult site, and from the adult to juvenile site, each locality hosts a complex size-structure formed from a mixture of younger and older shark individuals, and it is this mixture from which accumulated tooth distributions are derived.

We considered four key dynamics influencing changes in population size for both sites: reproduction, somatic growth, mortality, and dispersal between sites. We set juvenile/adult sites to be 700 Km [45,47] and 400 Km apart for Eocene sites, where seasonal fluctuations in temperature reached site-specific minimum (winter) and maximum (summer) extremes, allowing us to consider the effects of locations farther from and closer to the equator (temperature parameters are reported in the Results and Discussion). By simulating shark population dynamics we tracked changes in population size structure as reflected by teeth, which are strongly correlated with size [5]. A comparison of simulated body size distributions against those observed from different environments thus allows us to propose specific ecological mechanisms giving rise to observed features in empirical size structure, and the resulting accumulated dental distributions, from site to site. Because there is not significant sexual dimorphism among sand tigers [48], our model considers only the population dynamics of females.

In our framework, reproduction takes place only at the juvenile site, whereas mortality occurs at both sites. The per-capita reproductive rate $r$ was thus set to $r = 0$ at the adult site, and $r = 0.47 \times 10^{-7}$ female inds/s [49] at the juvenile site, independent from time of year or water temperature. The per-capita mortality rate was assumed to be constant across size classes within both juvenile and adult sites at $\mu = 5.71 \times 10^{-9}$ inds/s [18]. Shark individuals were assumed to increase in mass $m$ (g) following the growth trajectory described by West et al. [16] as a function of metabolic rate. Metabolism $B$ (W·g$^{-3/4}$, where W is watts) is partitioned between somatic

growth and maintenance, providing a general equation for ontogenetic growth trajectories [16,50–53]. Ontogenetic growth is derived from the balance condition $B_0(T)m^\eta = E_m\dot{m} + B_m(T)m$, where $E_m = 5774$ (J/g) is the energy needed to synthesize a unit of mass [50,52,54,55], $B_m(T)$ is the temperature (T)-dependent metabolic rate to support an existing unit of mass, $B_0(T)$ is the temperature-dependent metabolic normalization constant, and temperature is in Kelvin [16,50–53]. The time that it takes to reach size $m$ as an individual grows from the initial mass $m_0$ to the asymptotic adult mass $M$ is given by the timescale

$$\tau\left(m\right) = \ln\left[\frac{1-\left(m_0/M\right)^{1-\eta}}{1-\left(m/M\right)^{1-\eta}}\right]\frac{M^{1-\eta}}{\alpha(T)\left(1-\eta\right)}, \tag{2.1}$$

given $\alpha(T) = B_0(T)/E_m$, and the scaling exponent $\eta = 3/4$ [56]. Because contemporary and Eocene sand tigers are assumed to be ectotherms, we incorporate a temperature-dependence for metabolic parameters, such that $B_0(T) = \exp[C - E/kT]$, where the normalization constant $C = 18.47$ for fish, the activation energy $E = 0.63$ (eV; electron volts), and Boltzmann's constant $k = 8.6173 \times 10^{-5}$ (eV/Kelvin) [57]. Accordingly, shark individuals grow more quickly in warm environments, reaching the asymptotic mass $M$ at a younger age. We assume each site varies in temperature along a sinusoidal trajectory, from a summer maximum to a winter minimum and back over the course of a year, such that individuals in both juvenile and adult sites experience local seasonal variation in temperature as they migrate from site to site.

In our two-site model, juveniles disperse to the adult site once they have reached a particular mass, and adult females migrate annually from the adult to juvenile site to reproduce. The maximal migration rate is assumed to be a function of the distance between the nursery and the adult site, such that $d_{\max} = v/\delta$, where velocity $v = 1$ (m/s) and $\delta$ (m) is distance. The initial dispersal of juveniles to the adult site and annual dispersal of adults to the juvenile site are considered separately because we assume these events are mass-dependent and time-dependent, respectively. When newborns of size $m_0$ are born in the juvenile site, we assume they begin dispersing to the adult site at the threshold mass of $m_j = (1/4)M$ (g).

A strict juvenile dispersal strategy means that initial dispersal to the juvenile site occurs when individuals reach $m_j$. A flexible juvenile dispersal strategy means that dispersal may occur at sizes smaller or larger than $m_j$. If the initial dispersal rate of juveniles to the adult site $d_{j\to a}^{\text{initial}}(m)$ is mass-dependent, varying from $d = 0$ near $m_0$ and increasing sigmoidally to $d = d_j^{\max}$ above $m_j$, it can be described as

$$d_{j\to a}^{\text{initial}}(m) = \frac{d_j^{\max}}{1+\exp\left[\frac{-(m-m_j)}{\xi_j}\right]}, \tag{2.2}$$

where $\xi_j$ describes the flexibility of the size-dependent migration. In other words, as juveniles increase in size to $m_j$, their migration rate to the adult site increases sigmoidally to $d_{\max}$. Adults occupying the juvenile site disperse back to the adult site at a constant rate, having already attained $d_{\max}$. The juvenile dispersal window $\xi_j$ describes the flexibility of this mass threshold: a smaller dispersal window (low $\xi_j$) means that initial dispersal of juveniles to the adult site operates around a strict mass threshold $m_j$, whereas a large juvenile dispersal window (high $\xi_j$) means that initial dispersal of juveniles to the adult site is flexible around $m_j$. Importantly, a low juvenile dispersal window also implies that the juvenile site is serving a separate function than the adult site - in other words, the juvenile site is operating as a distinct nursery where juveniles must reside until a particular threshold size.

We assume that individuals occupying the adult site disperse back to the juvenile site to reproduce annually, such that the adult dispersal rate $d_{a\to j}^{\text{annual}}(t)$ is a function of time. Accordingly, the dispersal rate is maximized to $d_a^{\max}$ on a particular day each year $t_{\text{peak}}$, and decreases to zero in a Gaussian manner before and after. Annual adult dispersal from the adult site to the juvenile site is thus described as

$$d_{a\to j}^{\text{annual}}(t) = d_a^{\max}\exp\left[\frac{-\left(t-t_{\text{peak}}\right)^2}{2\xi_a^2}\right]. \tag{2.3}$$

The adult dispersal window $\xi_a$ describes the flexibility of this annual dispersal: a smaller dispersal window (low $\xi_a$) means that annual adult dispersal to the juvenile site operates around a strict peak day, whereas a large adult dispersal window (high $\xi_a$) means that annual adult dispersal to the juvenile site is flexible. We note that the resolution and range of juvenile and adult dispersal windows had to be adjusted from site to site to account for simulation limitations related to population dynamics in different temperature environments.

Because we aim to understand the shapes of dental distributions from the perspective of shark population dynamics, we must simulate the loss and accumulation of teeth over time in both juvenile and adult sites. We focus only on the loss of the first upper and lower anterior teeth (A1 and a1) to reflect those used to build the empirical distributions. To simulate accumulated dental distributions, we assumed a similar rate to *Triakis semifasciata* with a tooth loss rate of one upper and lower tooth every 40 days [58]; although this species differs from sand tigers, it is the only species with an experimentally controlled, quantitative measurement of tooth drop. This rate of tooth drop corresponds to $5.79 \times 10^{-7}$ teeth/s.

### (c) Comparing observed and simulated dental distributions

Our overall goal is to use the known conditions generating simulated dental distributions to gain insight into the unknown conditions generating empirical dental distributions. Specifically, we aim to evaluate *i*) whether an observed distribution is better described as a juvenile versus adult site, and *ii*) which dispersal strategy – strict versus flexible juvenile and adult dispersal windows – may have contributed to the observed distributional geometry. To compare simulated dental distributions to those observed from contemporary and Eocene localities, we first parameterized the model with estimated winter minimum and summer maximum mean ocean temperatures for both juvenile and adult sites. We then simulated dental distributions for both juvenile and adult sites across all combinations of $(\xi_j, \xi_a)$. Because simulated distributions were both non-normal and multi-modal, to compare distributions we compared means, standard deviations, and both the presence/absence and numerically-estimated values of one or multiple modes – into a single error term

$$\epsilon_{j,a}(\xi_j, \xi_a) = \sum_{k=1}^{4} \left| w_k^{\mathrm{sim}}(\xi_j, \xi_a) - w_k^{\mathrm{obs}} \right| / w_k^{\mathrm{obs}}, \tag{2.4}$$

for juvenile and adult sites, where $w_k^{\mathrm{sim}}(\xi_j, \xi_a)$ and $w_k^{\mathrm{obs}}$ are the measured values for the features described above with respect to simulated and observed tooth distributions respectively, given the simulated dispersal windows $(\xi_j, \xi_a)$. Accordingly, the simulated juvenile or adult site dental distribution with a lower $\epsilon$ will indicate a better match for the observed dental distribution, and the particular combination of $(\xi_j, \xi_a)$ that results in the lower $\epsilon$ will point to the best-fit dispersal strategy.

## 3. Results and Discussion

### (a) Discerning distributions of dentition

The life history and movement of extant sand tigers (*Carcharias taurus*) has been examined extensively in the western Atlantic, in particular the population near Delaware Bay. A long-standing tagging program led by Delaware State University and University of Delaware between 2007 to 2015 recorded biological information such as fork length, total length, sex, and maturity state, as well as annual/seasonal movement data via acoustic and satellite tagging [43–46]. Occupation of the Delaware Bay by sand tigers correlates strongly with temperature, with juveniles arriving approximately one month prior to adults [44,45]. The residence time for the majority of individuals on the order of 150 days and sharks disperse from the site once the temperatures decrease in October [44,45]. Tooth length was estimated from empirical measures of body length based on well-known allometric relationships [5,6]. We found the estimated mean

anterior tooth crown height for the Delaware Bay population to be 18.92 mm with a maximum of 26.11 mm, which corresponds with actual total body length of 213 cm and 295 cm, respectively. Previous work based on 96 sand tiger individuals revealed the asymptotic body length for this species to be 296 cm [48], similar to the maximum size estimated in the Delaware Bay.

The Eocene sites explored here are well-known and iconic in the paleontological literature. The Eureka Sound Fm. on Banks Island (Canada, figure 1, dark green) and La Meseta Fm. on Seymour Island (Antarctica, figure 1, dark blue) are the most fossiliferous high latitude Eocene sites, with previous studies focused on sedimentology, flora, and fauna [24,30,59–62]. In both sites, the extinct sand tigers are well represented as †*S. macrota* and another †*Carcharias* species [28,32]. The geology of the Eureka Sound Fm. on Banks Island (Canada) points to a coastal deltaic environment with low shark diversity during the Eocene [32], whereas the La Meseta Fm. on Seymour Island (Antarctica) is noted for its rich and diverse marine assemblage that includes 35 species of sharks [28]. Among low-latitude Eocene sites, the Bashi/Tuscahoma Fm. at the Red Hot Truck Stop (MS) is largely known for its mammalian record, and is preserved in a lithology that suggests a large-scale, fluvial-dominated deltaic system [35,36,63] (figure 1, light green). Fully marine habitats are rare across the Eocene Gulf of Mexico, however the Crockett Fm. at Whiskey Bridge (TX) is one of the most fossiliferous Eocene marine sites known [64](figure 1, light blue). While the Red Hot Truck Stop and Whiskey Creek Bridge localities are relatively proximal along the Gulf, they are not necessarily contemporaneous as the Bashi/Tuscahoma Fm. spans the Paleocene-Eocene Thermal Maximum [36,63] whereas the Crockett Fm. is Middle Eocene [64], and likely represent distinct sand tiger populations. The localities in this study represent different depositional environments and our model indicates these differences are important to the life history of sand tigers during the Eocene and today.

The large sample sizes of sand tiger teeth from the Eocene sites allows for population-level analyses in the fossil record, which is rare for vertebrate fossil assemblages. We measured a total of 1,053 anterior fossil sand tiger teeth across the four fossil sites (see Supplemental Table), with distinct distributional geometries characterizing each locality (figure 1. The Banks Island collection consisted of 397 anterior teeth with a mean ± SD crown height of 13.70 mm ± 3.41 (median = 14.10 mm). The Seymour Island collections consisted of 450 anterior teeth with mean crown height of 19.61 mm ± 6.39 (median = 18.00 mm). The Red Hot Truck Stop collection included 284 anterior teeth with mean crown height of 12.62 mm ± 3.82 (median = 12.10 mm). Finally, the Whiskey Bridge collection included 158 anterior teeth with mean crown height of 22.51 mm ± 4.59 (median = 22.55 mm). These sample sizes far exceed that required to estimate the distribution moments for each locality (Banks Island, n = 24; Seymour Island, n = 41; Red Hot Truck Stop, n = 35; Whiskey Bridge, n = 16). We find that the observed dental distributions characterizing each site are significantly different when compared against each other (one-way ANOVA: df = 3, F = 283. 74, $p<0.0001$; posthoc Tukey HSD: $p=0.001$).

We note that the two fossil localities representing open marine habitats – Seymour Island (Antarctica) and Whiskey Bridge (TX) – include the largest anterior teeth documented across contemporary and Eocene systems, measuring 41.00 mm and 32.57 mm, respectively. Assuming Eocene and extant sand tigers have similar tooth-body size allometric relationships, the largest teeth from Seymour Island and Whiskey Bridge correspond to body lengths measuring 486 cm and 381 cm at these high and mid-latitude sites, respectively. Larger body sizes of sand tigers in the Eocene may be an evolutionary adaptation towards different environmental/ecological conditions, but may also simply be due to ontogenetic plasticity fueled by warmer oceanic temperatures [10].

## (b) Dispersal drives diverse dental distributions

The results of our population simulation reveal that changes in the initial dispersal of younger sharks from the juvenile site to the adult site, and of older sharks from the adult to juvenile site, can drastically change the shape of dental distributions within both sites (figure 3). Specifically, we examine the effects of increasing flexibility in the onset of these different dispersal events,

where the initial migration of younger sharks to the adult site is a function of their mass ($\xi_j$; x-axis in figure 3) and adult migration to the juvenile site is a function of the time of year ($\xi_a$; y-axis in figure 3). We distinguish four quadrants capturing the range of variation in dental distribution geometries that result from different juvenile and adult dispersal strategies in figure 3 (regions I-IV). We emphasize that our simulation framework is designed to examine whether the dispersal strategies described are able to account for the variation observed among empirical dental distributions, in part due to the limited ecological information we have for extinct taxa from the fossil record. We cannot discount alternative influences such as those stemming from the effects of intra- and inter-specific competition, higher-trophic species interactions, or evolutionary drivers, which we do not examine here.

As dispersal windows increase, both the initial dispersal of juveniles to the adult site and the annual dispersal of adults to the juvenile site varies widely. For a shark with an asymptotic mass of 350 kg, where we assume maturity is reached at $m_j = 87$ kg, the initial migration to the adult site ranged from 0.5 kg around $m_j$ (low flexibility) to 87 kg around $m_j$, effectively meaning it can migrate at any time after birth (high flexibility). In contrast, adult dispersal back to the juvenile site is a function of time, and we allowed this dispersal window to vary from 1 day around the peak dispersal day (low flexibility) to up to 50 days around the peak dispersal day (high flexibility). With maximum flexibility in both juvenile and adult dispersal windows (high $\xi_j$ and $\xi_a$), we observe the fallen teeth accumulating at each site to converge towards a single distributional geometry at both sites (region II in figure 3), an effect of highly mixed juvenile and adult populations. As both dispersal windows decrease towards minimal flexiblity (low $\xi_j$ and $\xi_a$), we observe the dental distributions to become distinct, with a very low and very high mean tooth size in the juvenile and adult site, respectively (region III in figure 3), an effect of strict size-based and temporal dispersal constraints.

When initial juvenile and annual adult dispersal windows are asymmetric, the shapes of accumulated dental distributions at each site become less intuitive. If the size at which juveniles first disperse to the adult site is strict (small $\xi_j$) and the timing of adult migration varies widely (large $\xi_a$), we observe that *i*) the mean of the juvenile distribution is much lower than the mean of the adult distribution, and *ii*) the variance of the juvenile distribution is large while the variance of the adult distribution is small (region I, figure 3). Because juvenile dispersal is restricted, they cannot travel to the adult site until they reach $m_j$, lowering the representation of smaller size classes in the adult site. However, because adult dispersal is more flexible, there is increasing representation of adult size-classes in the juvenile site, increasing variability.

If the size at which juveniles first disperse to the adult site is variable (large $\xi_j$) and the timing of the adult migration is strict (small $\xi_a$), we observe *i*) the emergence of two distinct modes in the dental distributions accumulating at both sites, and *ii*) asymmetry in modal frequencies at the juvenile site where the smaller mode is emphasized, and more even modal frequencies at the adult site (region IV in figure 3). Bimodality in dental distributions generally occurs when adult dispersal is restricted ($\xi_a < 30$ days) but across a relatively large range of juvenile dispersal mass ($\xi_j > 50$ kg). Accordingly, the initial dispersal of juveniles is independent of size, while annual adult dispersal is more restricted.

There are two forces acting to promote bimodality. First, increased variability in juvenile body size initiating dispersal to the adult site results in greater representation of smaller size-classes at the adult site. Second, lower dispersal flexibility at the adult site means that individuals have a chance to grow in body size before they return to the juvenile site to reproduce, increasing differences in size-classes between the two sites. The frequency asymmetry at the juvenile site is largely due to an over-representation of offspring prior to initial dispersal.

Juvenile sharks may leave their natal site – often in shallow estuaries [21,47] – to less protected pelagic environments across a range of sizes and times, depending on the availability of resources and predation pressure [65]. Importantly, a juvenile site functions as a nursery if and only if there is a size threshold governing an individual's initial migration to the adult site. If migration out

of the nursery is fluid and independent of size, the site is assumed to no longer provide a size-dependent fitness advantage, such that a designation of 'nursery' is unmerited. We observe that variation in the onset of these dispersal events – the initial dispersal of juveniles to a pelagic adult site, and annual returns of adults to a juvenile site to reproduce – has profound effects on the shapes of shark tooth distributions accumulating at both sites. Having established this range of ecological drivers on distribution shape, we next examine whether and to what extent we can extract ecological meaning from the shape of an extant sand tiger size distribution, and then extend our approach to interpret the dental distributions from Eocene deposits.

## (c) A contemporary dental distribution predicts known dispersal strategies

While it is relatively straightforward to show how different life history characteristics may influence distributions of accumulated shark teeth by forward-simulation, it is a more difficult prospect to start with a distribution and attempt to back-calculate some understanding of the potential ecological drivers from which it emerged. Considering only the dispersal strategies assessed here, we have shown that variation in dispersal windows results in a complex array of distributional geometries, so it is not a given that we can extract insight from the distribution alone. We next examine whether and to what extent we can gather ecological insight (i.e., dispersal and or migration timing) into a well-known contemporary sand tiger population based on our established framework.

Extant sand tiger sharks (*C. taurus*) are highly migratory along the continental shelf of the western margin of the Atlantic Ocean [44,45,47,66]. In the Delaware Bay, sand tigers aggregate in the summer to fall, and include a mixture of both juvenile and adult size classes [44,45]. The proposed nursery for sand tigers in the western Atlantic is the Plymouth, Kingston, Duxbury Bay (MA) where individuals span 78-104 cm (ATCH range 8.3 – 10.4cm) [47], substantially smaller and younger than individuals in Delaware Bay. As such, the Delaware Bay aggregate is thought to represent a mixed age population at an adult site, where dispersal to the the Bay corresponds closely with seasonal temperature [45]. Acoustic tagging efforts indicate a gradual arrival of sand tigers, where juveniles begin arriving in early May with adults arriving approximately one month later [44]. In contrast to their arrival, the departure window at Delaware Bay is more tightly constrained from early to mid-October [44,45]. Most individuals are present in the Bay for ca. 150 days, which is roughly a 40 day standard deviation around peak the migration time [44]. The migration distance for sand tigers from the Delaware Bay to more warmer waters of North Carolina to Florida is 200-600 km [45], however, in Australia *C. taurus* is known to migrate up to 1500 km [67]. This well-studied modern sand tiger population at Delaware Bay thus provides a distinct opportunity to examine whether certain aspects of the well-known life-histories can be disentangled from the distributions alone.

To capture conditions representative of the migratory environment experienced by sand tigers along the Massachusetts to Delaware coastline, we set the minimum and maximum temperatures of the simulated juvenile site to 17°C and 25°C, and the minimum and maximum temperatures of the simulated adult site to 13°C and 23°C [44,45,47], where we assumed a distance of 700 Km separating sites. We then systematically compared the dental distributions produced by our population simulation across values of $\xi_j$ and $\xi_a$ for both juvenile and adult sites against the empirical distribution from the Delaware Bay by estimating error in model fit $\epsilon$ (equation 2.4). We compare the model fit error for both the simulated juvenile and adult sites ($\epsilon_j$ versus $\epsilon_a$) by first investigating whether our framework was capable of detecting if the Delaware Bay population more likely represented a juvenile versus adult site. Our assessment reveals that the minimal error for the juvenile site is $\epsilon_j = 0.6$, whereas the minimal error for the adult site is $\epsilon_a = 0.25$ (figure 4). This suggests that the Delaware Bay population represents an adult rather than juvenile population, confirming what is already understood [44,47], but more importantly – at broad strokes – validating the usefulness of our approach.

Except for the scenarios where dental distributions are very similar (high $\xi_j$ and $\xi_a$) or bimodal (high $\xi_j$ and low $\xi_a$), site identity is relatively straightforward to distinguish based on differences

in tooth size means. A more rigorous assessment of our approach is to examine whether the best fit parameterization of dispersal windows $(\xi_j, \xi_a)$ correlates with our understanding of the Delaware Bay system. We find that, given the adult site identification of the Delaware Bay population, the best fit dispersal window parameterization indicates a strict mass at which juveniles leave for the adult site ($\xi_j = 1$) and a flexible temporal window describing the annual adult migration ($\xi_a = 40$). Importantly, the temporal range that describes the arrival of adults to Delaware Bay – a standard deviation of ca. 40 days around the peak arrival date [44] – closely matches the expected adult dispersal window predicted by our best-fit model distribution (figure 4). And while we do not have information on the range of mass classes initiating first dispersal to Delaware Bay, the low juvenile dispersal window provides indirect support for the Plymouth, Kingston, Duxbury Bay juvenile site functions as a nursery where pups remain until a strict size threshold is reached. By matching the observed Delaware Bay dental distribution to those simulated from established conditions, we suggest that our framework may provide insight into central life history characteristics governing sand tiger dispersal.

## (d) Deciphering life history and dispersal in the Eocene

Understanding the nature of shark communities in response to documented changes in Eocene climate may provide insight into the future of shark populations in our changing oceans. Because our primary window into these systems is through the lens of accumulated teeth, interpreting dental distributions from an ecological perspective may permit disentangling aspects of their ecologies, such as life history mediated dispersal behaviors. Informing our population simulation with ocean temperatures experienced by sand tigers in the Eocene, we use our framework to examine the underlying ecological constraints potentially driving the accumulation of dental distributions at two high latitude and two low latitude Eocene sites.

High latitude locations include the Banks Island (Canada) brackish and Seymour Island (Antarctic) marine sites, whereas low latitude locations include the Red Hot Truck Stop (MS) estuary and Whiskey Creek (TX) marine sites. Reconstruction of temperature regimes vary from high- to low-latitude sites. High-latitude sites have more extreme summer highs and winter lows with exaggerated differences between coastal and pelagic environments, with brackish (juvenile site) habitats ranging from $12^{\circ}$C to $24^{\circ}$C [68–71] and marine (adult site) habitats ranging from $9^{\circ}$C to $17^{\circ}$C [10,70–72]. In contrast, low-latitude sites have more equitable summer highs and winter lows with less extreme differences between coastal and pelagic environments, with both brackish and marine habitats ranging from $23^{\circ}$C to $30^{\circ}$C [73,74]. For all Eocene localities, we set the distance between juvenile and adult sites to 400 Km. While we do not know the actual distances separating juvenile and adult sites in the Eocene, even large differences in distance have negligible effects on tooth distributions (e.g. $\pm 150 Km$ differences in distance result in $< 1\%$ change in distributional means; supplementary figure 1). Throughout we assume similar vital rates controlling shark growth and reproduction in both modern and Eocene localities.

Given the reconstructed temperature regimes for high- and low-latitude Eocene sites, results from simulated dental distributions revealed qualitatively similar geometries across $\xi_j$ and $\xi_a$. For example, warmer temperatures in low-latitude sites reduce the prevalence of bimodality at juvenile sites (region IV in figure 3 and supplementary figures 2,3) and accumulated tooth size is generally more variable in warmer environments (all regions in figure 3 and supplementary figures 2-3). In warmer sites, shark growth rate is increased (Eq. 2.1), allowing individuals to reach maturity faster, resulting in larger populations that are composed of more individuals with larger body size. The increase in overall variability is due to this broader range of size classes, whereas the reduced bimodality with high $\xi_j$ and low $\xi_a$ at the juvenile site is due to the accumulation of younger individuals quickly reaching larger body size prior to initial dispersal to the adult site.

We next use our simulated Eocene dental distributions to gain insight into whether high- and low-latitude localities are expected to represent juvenile or adult sites. Our evaluation of sand tiger size structure from both high- and low-latitude brackish and marine sites aligns with paleontological reconstructions of site habitat. For high-latitude locations, we observe that the

Banks Island (Canada) site better fits the simulated juvenile ($\epsilon_j = 0.62$) relative to adult site ($\epsilon_a = 1.32$), whereas the Seymour Island (Antarctica) site better fits the simulated adult ($\epsilon_a = 0.29$) relative to juvenile site ($\epsilon_j = 0.31$), though this latter difference is negligible (rows 1-2, figure 5). In comparison, the fossil shark tooth-bearing strata of Banks Island (Eureka Sound Fm.) dates to the early-middle Eocene [32,75–78], and is reconstructed to be a channel or mouth bar deposit of a delta front [77]. The presence of sand tiger teeth in unconsolidated sands, a fossilized crocodyliform fossil [79], and paleosalinity reconstructed to be much lower than today's Arctic surface waters [8,23], all point to a mild and brackish estuarine environment [70,71], supporting the our finding of this site representing a nursery location (row 1, figure 5). In contrast, the faunal composition and geochemistry of the Seymour Island locality (La Meseta Fm.) suggest typical marine conditions [10,26,28,80,81]. This site encompasses seven stratigraphic biostratigraphy units (TELM; Tertiary Eocene La Meseta) that span middle to late Eocene; although the shark assemblage changes within each TELM [28], *S. macrota* is the most abundant and represented in TELMs 3-5 that span 45-41 My [10,82,83]. Temperature reconstructions and climate simulations point to relatively warm and stable conditions [10,72], though tectonic models indicate early opening of the Drakes Passage [84] that had large effects on paleoceanographic conditions [85]. While our simulations support this locality serving as an adult site, the plateaued error surface precludes a clear interpretation (row 2, figure 5).

For low-latitude localities, we observe that the Red Hot Truck Stop (MS) better fits simulated juvenile ($\epsilon_j = 0.21$) compared to adult sites ($\epsilon_a = 1.96$), whereas Whiskey Creek (TX) better fits simulated adult ($\epsilon_a = 1.03$) compared to juvenile sites ($\epsilon_j = 2.03$) (rows 3-4, figure 5. Palynofloral reconstruction of the Red Hot Truck Stop locality (Bashi/Tuscahoma Fm.) supports a paratropical climate [86] characterized by a large fluvial-dominated deltaic system in an estuarine habitat that spans the Paleocene/Eocene Thermal Maximum [35,36,63]. In contrast, the Whiskey Creek locality (Crockett Fm.) is dated to the early part of the Middle Eocene Climate Optimum (MECO)[64] and represents a shallower marine habitat with normal salinity [37,38]. This sub-tropical climate supported at least three species of sand tiger sharks ($^{\dagger}$*Carcharias cuspidata*, $^{\dagger}$*C. hopei*, and $^{\dagger}$*S. macrota*) [34,37] found within the Stone City Member of the Crockett Fm. Taken together, these reconstructions support the notion that Red Hot Truck Stop and Whiskey Creek represent juvenile and adult sites respectively, as predicted by our model results.

## (e) Dental distributions support the importance of shark nurseries

Contemporary sand tiger size structure suggest strict juvenile dispersal windows (low $\xi_j$) and flexible adult dispersal windows (high $\xi_j$; figure 4). However, best fit simulated dental distributions for both high- and low- latitude brackish and marine Eocene localities all point to adult dispersal windows that are either intermediate (the Banks Island brackish locality, and the Seymour Island and Whiskey Ridge marine localities) or very small (the Red Hot Truck Stop brackish locality). If the adult dispersal window is small, annual adult migration to juvenile sites is restricted, pointing to stronger effects of seasonality on sand tiger life history. Paleoclimate reconstruction of the Eocene Arctic does indicate strong seasonality with a temperature shift of $16.5^{\circ}$C between summer and winter with cold month mean temperatures over $0^{\circ}$C while warm month mean temperature estimates span $19 - 25^{\circ}$C [69–71,87,88], and this would suggest sharks in these environments may have life histories that are strongly seasonal. Moreover, the oxygen isotopic record of *Conus* shells along the Gulf Coast points to seasonal changes in nutrient availability [89], where spring upwelling likely facilitated increased productivity. Taken together, our results support a significant effect of seasonality driving dispersal to juvenile sites for both high- and low-latitude Eocene localities, in line with expectations from the geological record.

The contemporary Delaware Bay sand tiger population as well as those from all Eocene sites except the Seymour Island marine locality point to a small juvenile dispersal window, meaning that a strict size threshold initiates first dispersal to the adult site (figure 5). With regard to the Seymour Island locality, we observe that, for both simulated juvenile and adult sites, the error surface uniquely plateaus across a large range of potential $(\xi_j, \xi_a)$ values providing similarly

good fits (row 2 in figure 5). This error surface limits our ability to either interpret whether Seymour Island better represents a juvenile versus adult site or to confidently estimate the size of either dispersal window. Elevated juvenile and adult dispersal windows in the Antarctic may not be surprising, as this site is known to have accumulated across a longer temporal window [90] where changing environmental conditions associated with the opening of the Drake passage [10,72] affected the shark community assembly [28] and may have influenced how sites were used by shark populations over time and space.

Contemporary shark nurseries are thought to enable resource access, promote juvenile growth, and to protect vulnerable pups against mortality from potential predators [19,21,47]. Upon maturation and release from mesopredator pressure, dispersal to adult sites enables growing individuals access to larger prey and perhaps mating opportunities [91], though the timing of these events are variable among sand tiger populations [45,66,67,92]. In our framework, a large juvenile dispersal window means that both smaller and larger individuals initiate this first dispersal. These conditions imply that the costs and benefits of the juvenile site are similar to those of the adult site, such that it is no longer serving in the context of a nursery. In contrast, a strict juvenile dispersal window points to a sharp threshold in body size initiating first dispersal, implying that the costs and benefits in juvenile and adult sites vary significantly. This scenario means that the juvenile site is playing an important role in structuring shark life history, supporting the notion of the locality serving as a nursery.

We find strong support for strict juvenile dispersal windows and by extension strong support for the role of juvenile sites serving as nurseries for the contemporary sand tiger population as well as three of four Eocene localities. This result supports the notion that nurseries are a vital component of sand tiger life histories, present across a range of oceanic conditions and spanning tens of millions of years. Declines in nursery habitats have been invoked as a potential extinction mechanism for both fossil [12] and contemporary shark populations [19,21,93], though the extent to which nurseries may buffer against population declines is controversial [94]. By linking dental distribution shape to strict juvenile dispersal windows, our results lend strong support for the presence of nurseries and their utmost importance to maintain sand tiger populations, both past and present.

## 4. Conclusion

We have shown that two important drivers of shark life history – the variability in the size of juveniles first leaving a nursery and the temporal variability marking annual migrations of adults back to a nursery – can result in the diversity of dental distributions characterizing both observed contemporary and paleontological sand tiger populations. We suggest that our framework provides mechanistic insight into whether a particular dental distribution is the product of either juvenile or adult site occupation, as well as particular life history attributes contributing to distributional geometries. Extending our framework to Eocene dental records, we find strong support for seasonal migrations to nursery localities, emphasizing the importance of nurseries in structuring the life histories of sand tigers over the course of their long evolutionary history.

Dental distributions directly reflect variability in body size, and it is this window into growth coupled with demography and dispersal strategies that permit insight into life history. Body size distributions are naturally reflections of ontogenetic and demographic processes within populations, and different shark species are characterized by distributions with distinct shapes. For example, great white sharks (*Carcharodon carcharias*), bluntnose sixgill sharks (*Hexanchus griseus*), and greenland sharks (*Somniosus microcephalus*) have body size distributions that appear normally distributed, whereas basking sharks (*Cetorhinus maximus*) tend towards bimodal distributions [95], megamouth sharks (*Megachasma pelagios*) have distributions that are right-skewed [96], and some extinct sharks (*Otodus megalodon*) had body size distributions that appear left-skewed [97]. Understanding the drivers of these body size distributions, measured directly

or estimated from tooth length, has the potential to reveal important insights into the ecological constraints shaping these systems.

While we evaluate the dental distributions treated here as a product of dispersal patterns driven largely by size and seasonality, the diverse distributions observed across shark species may also account for differences in survivorship, sexual dimorphism, and species' position within the marine food web. Because fossil teeth are accumulated over long periods of time, differences in some dental distributions may also reflect sediment formation, taphonomic dynamics, evolutionary change, and/or tectonic processes [98,99]. Disentangling the potential drivers of particular dental distributions must be justified from an understanding of both the geological characteristics of the locality as well as a biological understanding of the species. Deciphering the mechanisms from which dental distributions are formed permits an ecological window into both extinct and extant shark communities, and we suggest this may generate new insights into how these enduring and enigmatic species persist in the face of change.

Ethics. The authors have no competing interests to declare. All data and analyses provided here are not published elsewhere.

Data Accessibility. Raw data for empirical tooth distributions are provided in the Dryad repository XXX. Simulation code is available in the public GitHub repository https://github.com/jdyeakel/sharks_bodysize

Authors' Contributions. Conceptualization - SLK, JDY, JJE; Methodology - SLK, JDY, JJE; Investigation - SLK, JDY, SSZ, DF, JK; Formal Analysis - MAB, JDY, DF; Writing original draft - SLK, JDY, MAB; Review and Editing - all authors; Supervision - SLK, JJE; Funding Acquisition - SLK, JJE, JK.

Competing Interests. The authors have no competing interests.

Funding. This research was funded in part by the National Science Foundation (SGP1842049) and University of Chicago T.C. Chamberlin Fellowship to SLK; Mellon Mayes Undergraduate Fellowship at University of Chicago, National Science Foundation Graduate Research Fellowship, and NASA Emerging Worlds grant ($18-EW18_2-0084$) to SSZ; Austrian Science Fund (FWF) [P 33820] to JK. For the purpose of open access, JK has applied a CC BY public copyright licence to any Author. Field research to collect shark teeth on Banks Island, Canada was supported by National Science Foundation grant ARC0804627 to JE.

Acknowledgements. This research would not be possible without the support of many individuals. We thank the curators and collection managers for their help and access to collect the empirical data: K. Shepherd and M. Currie at the Canadian Museum of Nature, P. Holroyd at the University of California Museum of Paleontology, L. Skibinski at Paleontological Research Institute, T. Mörs at the Swedish Natural History Museum, A. Henrici at the Carnegie Museum of Natural History, and C. Flis at the Whiteside Natural History Museum. We are grateful to D. Fox for access to data from the 2012 *Carcarias taurus* tagging season as part of his research program at Delaware State University. Our research benefited from conversations with M. Clementz, P. Holroyd, D. Jablonski, and S. Kidwell over the years. Thank you to Christina Spence Morgan for scientific illustration on figures 1 and 2.

Disclaimer. Insert disclaimer text here.

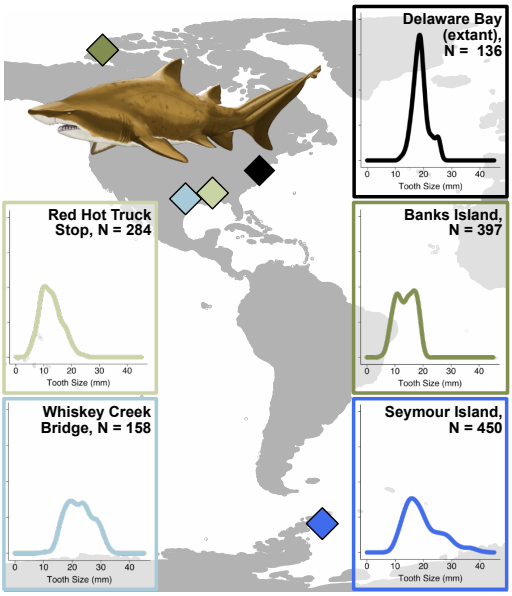


Figure 1: Map of sand tiger shark localities and their size distributions. Extant sand tiger sharks were caught at a mid-latitude marine site, Delaware Bay (black), where total length was measured and transformed to anterior tooth crown height. Eocene site size distributions are based on anterior tooth crown measurements. During the Eocene, the extinct *Striatolamia macrota* inhabited both high latitude waters (darker shades), such as Banks Island in the Canadian Arctic (Eureka Sound Fm., dark green), Seymour Island off the Antarctic Peninsula (La Meseta Fm., dark blue) and mid-latitude waters (lighter shades) in the Gulf of Mexico, such as the Red Hot Truck Stop in Mississippi (Bashi/Tuscahoma Fm., light green) and Whiskey Bridge in Texas (Crockett Fm., light blue). In addition to paired latitude, these sites were also chosen to represent brackish (Banks Island, high latitude, and Red Hot Truck Stop, low latitude; greens) and marine (Seymour Island, high latitude, and Whiskey Bridge, low latitude; blues) waters. †*Striatolamia macrota* illustration by Christina Spence Morgan.

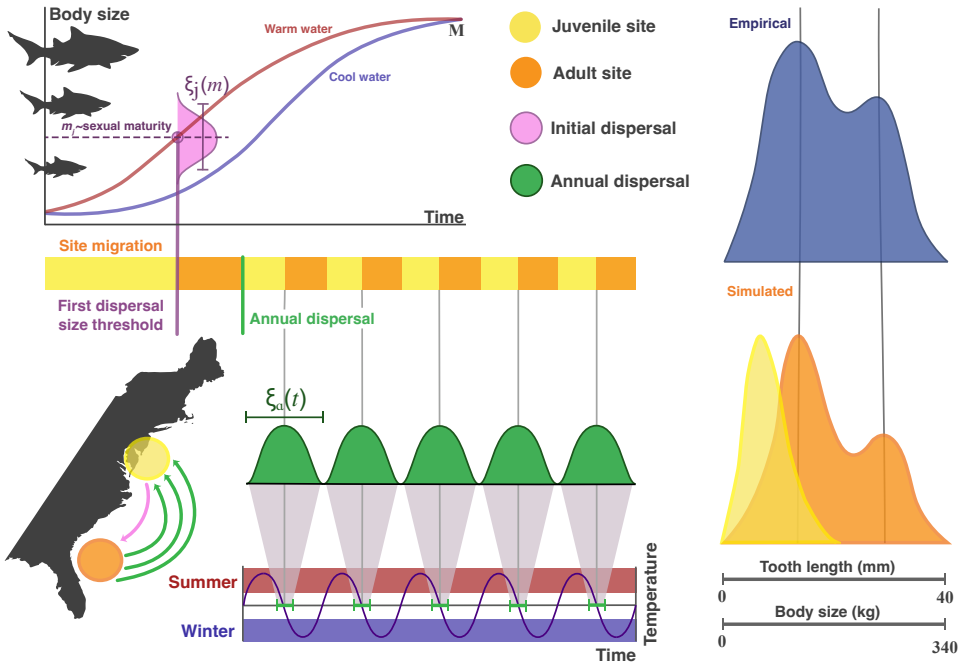


Figure 2: Conceptual diagram of the population simulation where sand tiger shark individuals migrate between a juvenile site or nursery (yellow) and adult site (orange). The ontogenetic growth rates of sand tiger individuals increase with temperature (blue and red growth curves) from an initial mass $m_0$ to an asymptotic mass $M$. After birth, newborns reside in the juvenile site until they reach maturity at mass $m_j$, after which they disperse to the adult site. The juvenile dispersal window $\xi_j$ (pink) denotes the variability in size at which initial dispersal occurs. Adults disperse to the juvenile site, where $\xi_a$ denotes the variability in the timing of the migration (green), which occurs annually from the adult to the juvenile site and back (map inset). Individuals drop teeth as they migrate, such that accumulating dental distributions capture the size structure of populations at both sites. Empirical dental distributions (blue distribution) can be compared to simulated distributions at juvenile and adult sites (yellow and orange distributions, respectively) and evaluated for best-fit based on mean, variance, and modality, thereby gaining insight into life-history characteristics such as the juvenile and adult dispersal windows. Illustration by Christina Spence Morgan.

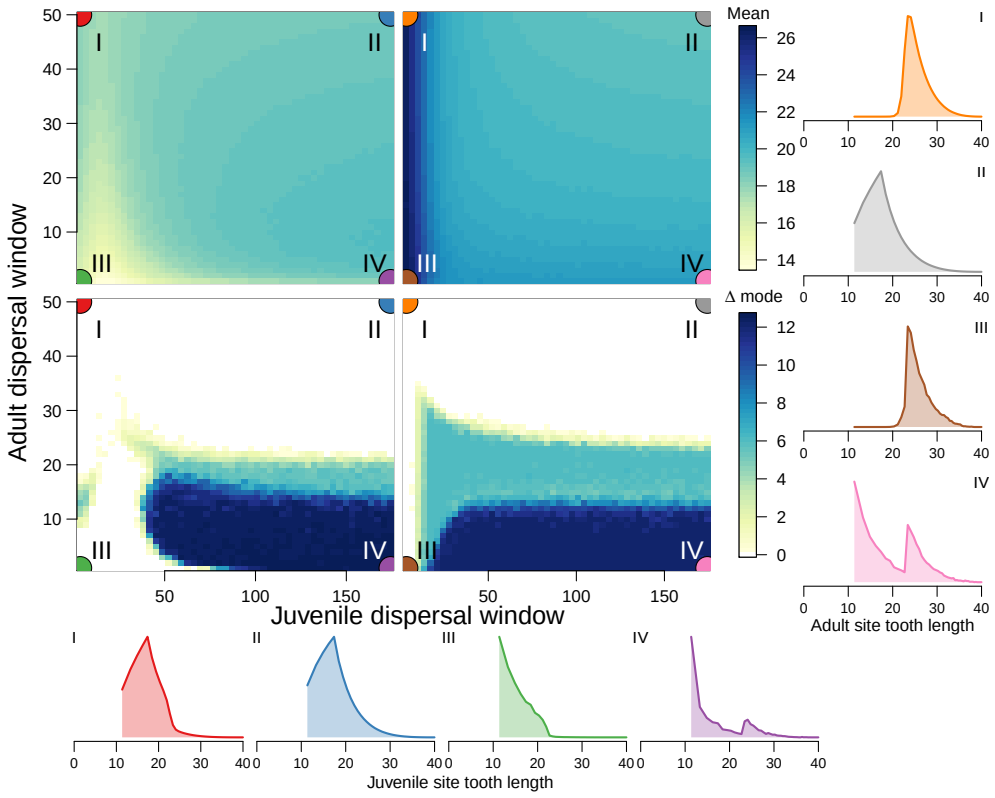


Figure 3: Simulation results for the dynamic population model as a function of juvenile and adult dispersal windows ($\xi_j$ and $\xi_a$, respectively). Changes in dental distribution shape are captured by site-specific means (top two panels) and the distance between modes ($\Delta$ mode; bottom two panels). A $\Delta$ mode value of zero means there is only one mode. Representative distributions of anterior tooth crown height are shown for juvenile site and adult sites for regions I-IV (horizontal along bottom and vertical along right edge, respectively), where color denotes both region and site identity. Regions I-IV depict various combinations of small and large dispersal windows. Region I (high $\xi_a$, low $\xi_j$); II (high $\xi_a$, high $\xi_j$); III (low $\xi_a$, low $\xi_j$); IV (low $\xi_a$, high $\xi_j$). Results are shown for high altitude Eocene conditions, but are qualitatively similar for all evaluated localities.

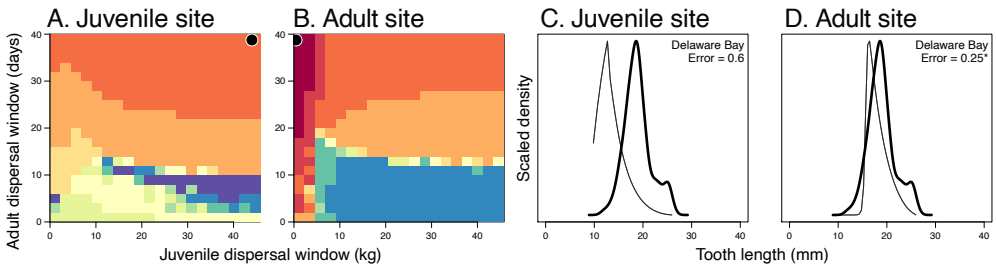


Figure 4: Comparison of empirical dental distributions from sand tigers in the Delaware Bay and those simulated across different values of the juvenile ($\xi_j$) and adult ($\xi_a$) dispersal windows. Better fits between empirical and simulated distributions at juvenile (A) and adult sites (B) are represented by warmer colors (lower $\epsilon$; Eq. 2.4). Best-fit simulation results for juvenile and adult simulation results at a particular $(\xi_j, \xi_a)$ are denoted by black circles. The corresponding distributions at this best-fit value of $(\xi_j, \xi_a)$ are shown for juvenile (C) and adult (D) sites for comparison (thin lines) relative to the empirical distribution (thick line). Within-site best-fit error values are reported in the upper-right, and the across-site best-fit error is denoted with an asterisk ($^*$).

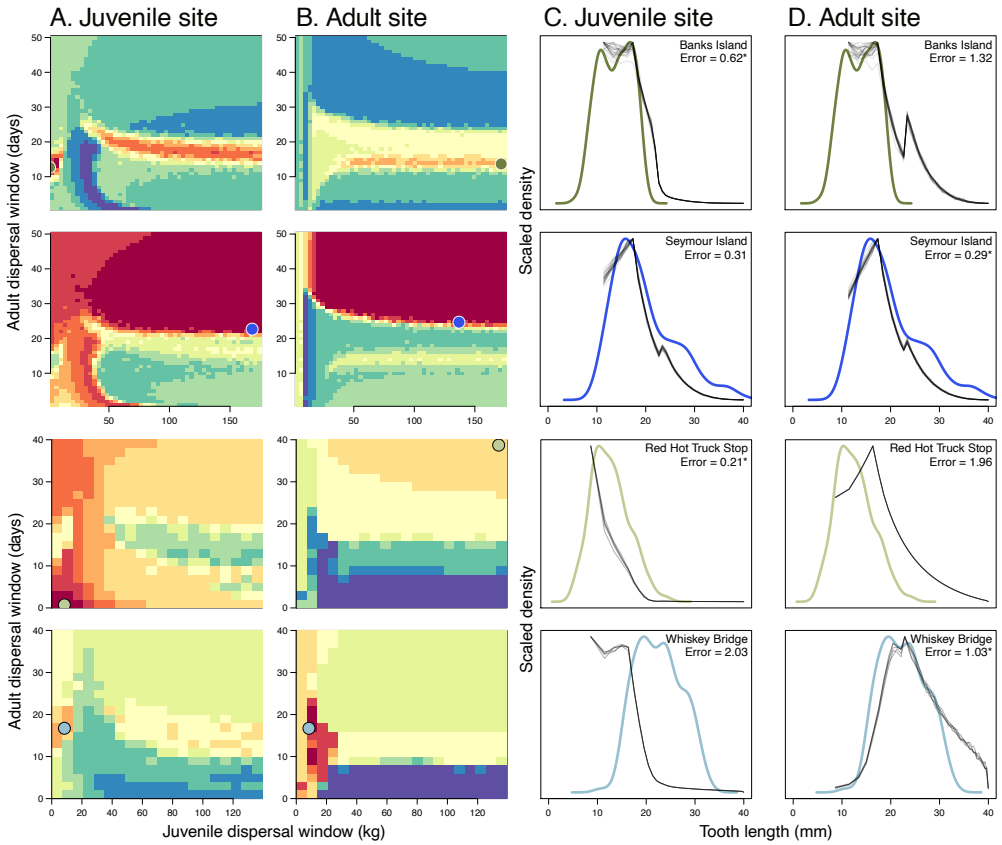


Figure 5: Comparison of empirical dental distributions from sand tigers at Eocene localities and those simulated across different values of the juvenile ($\xi_j$) and adult ($\xi_a$) dispersal windows. Eocene localities include the high latitude Banks Island (first row, dark green) and Seymour Island (second row, dark blue) sites as well as the low latitude Red Hot Truck Stop (third row, light green) and Whiskey Bridge Sites (fourth row, light blue). Blues denote sites reconstructed as marine habitats; greens denote sites reconstructed as near-shore estuarine habitats. Across all rows, better fits between empirical and simulated distributions at juvenile (A) and adult sites (B) are represented by warmer colors (lower $\epsilon$; Eq. 2.4). Best-fit simulation results for juvenile and adult simulation results at a particular $(\xi_j, \xi_a)$ are denoted by colored circles. The corresponding distributions at this best-fit value of $(\xi_j, \xi_a)$ are shown for juvenile (C) and adult (D) sites for comparison (thin lines) relative to the empirical distribution (thick line). Within-site best-fit error values are reported in the upper-right, and the across-site best-fit error is denoted with an asterisk ($^*$).

## References


1. Sibert E, Friedman M, Hull P, Hunt G, Norris R. 2018 Two pulses of morphological diversification in Pacific pelagic fishes following the Cretaceous–Palaeogene mass extinction. *Proceedings of the Royal Society B* **285**, 20181194.
2. Sibert EC, Rubin LD. 2021 An early Miocene extinction in pelagic sharks. *Science* **372**, 1105–1107.
3. Naylor GJ, de Lima A, Castro JI, Hubbell G, de Pinna MC. 2021 Comment on "An early Miocene extinction in pelagic sharks". *Science* **374**, eabj8723.
4. Feichtinger I, Adnet S, Cuny G, Guinot G, Kriwet J, Neubauer T, Pollerspöck J, Shimada K, Straube N, Underwood C et al.. 2021 Comment on "An early Miocene extinction in pelagic sharks". *Science* **374**, eabk0632.
5. Shimada K. 2002 Dental homologies in lamniform sharks (Chondrichthyes: Elasmobranchii). *Journal of Morphology* **251**, 38–72.
6. Shimada K. 2004 The relationship between the tooth size and total body length in the sandtiger shark, Carcharias taurus (Laminformes : Odontaspidae). *Journal of Fossil Research* **37**, 76–81.
7. Shimada K. 2007 Skeletal and dental anatomy of lamniform shark, Cretalamna appendiculata, from Upper Cretaceous Niobrara Chalk of Kansas. *Journal of Vertebrate Paleontology* **27**, 584–602.
8. Kim SSL, Eberle JJJ, Bell DDM, Fox DDA, Padilla A. 2014 Evidence from shark teeth for a brackish Arctic Ocean in the Eocene greenhouse. *Geology* **42**, 695–698.
9. Zacke A, Voigt S, Joachimski MM, Gale AS, Ward DJ, Tütken T. 2009 Surface-water freshening and high-latitude river discharge in the Eocene North Sea. *Journal of the Geological Society* **166**, 969–980.
10. Kim SL, Zeichner SS, Colman AS, Scher HD, Kriwet J, Mörs T, Huber M. 2020 Probing the ecology and climate of the Eocene Southern Ocean with sand tiger sharks Striatolamia macrota . *Paleoceanography and Paleoclimatology* pp. 1–21.
11. Straube N, Pollerspöck J. 2020 Intraspecific dental variations in the deep-sea shark Etmopterus spinax and their significance in the fossil record. *Zoomorphology* **139**, 483–491.
12. Pimiento C, Ehret DJ, MacFadden BJ, Hubbell G. 2010 Ancient nursery area for the extinct giant shark megalodon from the Miocene of Panama. *PLoS ONE* **5**.
13. Herraiz JL, Ribé J, Botella H, Martínez-Pérez C, Ferrón HG. 2020 Use of nursery areas by the extinct megatooth shark Otodus megalodon (Chondrichthyes: Lamniformes). *Biology letters* **16**, 20200746.
14. Villafaña JA, Hernandez S, Alvarado A, Shimada K, Pimiento C, Rivadeneira MM, Kriwet J. 2020 First evidence of a palaeo-nursery area of the great white shark. *Scientific Reports* **10**, 1–8.
15. Brose U, Jonsson T, Berlow EL, Warren P, Banasek-Richter C, Bersier LF, Blanchard JL, Brey T, Carpenter SR, Blandenier MFC et al.. 2006 Consumer–resource body-size relationships in natural food webs. *Ecology* **87**, 2411–2417.
16. West GB, Brown JH, Enquist BJ. 2001 A general model for ontogenetic growth. *Nature* **413**, 628–631.
17. Bhat U, Kempes CP, Yeakel JD. 2020 Scaling the risk landscape drives optimal life-history strategies and the evolution of grazing. *Proceedings of the National Academy of Sciences* **117**, 1580–1586.
18. Schindler DE, Essington TE, Kitchell JF, Boggs C, Hilborn R. 2002 Sharks and tunas: fisheries impacts on predators with contrasting life histories. *Ecological Applications* **12**, 735–748.
19. Heithaus MR. 2007 Nursery areas as essential shark habitats: a theoretical perspective. In *American Fisheries Society Symposium* vol. 50 p. 3. American Fisheries Society.
20. Doan MD, Kajiura SM. 2020 Adult blacktip sharks (Carcharhinus limbatus) use shallow water as a refuge from great hammerheads (Sphyrna mokarran). *Journal of fish biology* **96**, 1530–1533.
21. Heupel MR, Carlson JK, Simpfendorfer CA. 2007 Shark nursery areas: concepts, definition, characterization and assumptions. *Marine Ecology Progress Series* **337**, 287–297.
22. Burke KD, Williams JW, Chandler MA, Haywood AM, Lunt DJ, Otto-Bliesner BL. 2018 Pliocene and Eocene provide best analogs for near-future climates. *Proceedings of the National Academy of Sciences* **115**, 13288–13293.

23. Waddell LM, Moore TC. 2008 Salinity of the Eocene Arctic Ocean from oxygen isotope analysis of fish bone carbonate. *Paleoceanography* **23**, 1–14.
24. Greenwood DR, Basinger JF, Smith RY. 2010 How wet was the Arctic Eocene rain forest? Estimates of precipitation from Paleogene Arctic macrofloras. *Geology* **38**, 15–18.
25. Padilla A, Eberle JJ, Gottfried MD, Sweet AR, Hutchison JH. 2014 A sand tiger shark–dominated fauna from the Eocene Arctic greenhouse. *Journal of Vertebrate Paleontology* **34**, 1307–1316.
26. Ivany LC, Lohmann KC, Hasiuk F, Blake DB, Glass A, Aronson RB, Moody RM. 2008 Eocene climate record of a high southern latitude continental shelf: Seymour Island, Antarctica. *Bulletin of the Geological Society of America* **120**, 659–678.
27. Long DJ. 1992 Sharks from the La Meseta Formation (Eocene), Seymour Island, Antarctic Peninsula. *Journal of Vertebrate Paleontology* **12**, 11–32.
28. Kriwet J, Engelbrecht A, Mörs T, Reguero M, Pfaff C. 2016 Ultimate Eocene (Priabonian) chondrichthyans (Holocephali, Elasmobranchii) of Antarctica. *Journal of Vertebrate Paleontology* **36**.
29. Kriwet J. 2005 Additions to the Eocene selachian fauna of Antarctica with comments on Antarctic selachian diversity. *Journal of Vertebrate Paleontology* **25**, 1–7.
30. Reguero MA, Marenssi SA, Santillana SN. 2012 Weddellian marine/coastal vertebrates diversity from a basal horizon (Ypresian, Eocene) of the Cucullaea I Allomember, La Meseta formation, Seymour (Marambio) Island, Antarctica. *Rev. peru. biol.* **19**, 275–284.
31. Engelbrecht A, Mörs T, Reguero MA, Kriwet J. 2019 Skates and rays (Elasmobranchii, Batomorphii) from the Eocene La Meseta and Submeseta formations, Seymour Island, Antarctica. *Historical Biology* **31**, 1028–1044.
32. Padilla A, Eberle JJ, Gottfried MD, Sweet AR, Hutchison JH. 2014 A sand tiger shark-dominated fauna from the Eocene Arctic greenhouse. *Journal of Vertebrate Paleontology* **34**, 1307–1316.
33. Purdy RW. 1998 Chondrichthyan fishes from the Paleocene of South Carolina. *Transactions of the American philosophical society* pp. 122–146.
34. Westgate JW. 2001 Paleoecology and biostratigraphy of marginal marine Gulf Coast Eocene vertebrate localities. In *Eocene biodiversity* , pp. 263–297. Springer.
35. Ingram S. 1991 The Tuscahoma-Bashi section at Meridian, Mississippi: First notice of lowstand deposits above the Paleocene–Eocene TP2/TE1 sequence boundary. *Mississippi Geology* **11**, 9–14.
36. Beard KC, Dawson MR. 2009 Early Wasatchian mammals of the red hot local fauna, uppermost Tuscahoma formation, Lauderdale County, Mississippi. *Annals of Carnegie Museum* **78**, 193–243.
37. Breard SQ, Stringer GL. 1999 Abstract: Integrated Paleoecology and Marine Vertebrate Fauna of the Stone City Formation (Middle Eocene), Brazos River Section, Texas . *AAPG Bulletin* **83**.
38. Harding SC, Nash BP, Petersen EU, Ekdale A, Bradbury CD, Dyar MD. 2014 Mineralogy and geochemistry of the Main Glauconite Bed in the Middle Eocene of Texas: Paleoenvironmental implications for the Verdine Facies. *PloS one* **9**, e87656.
39. Jorgensen SJ, Reeb CA, Chapple TK, Anderson S, Perle C, Van Sommeran SR, Fritz-Cope C, Brown AC, Klimley AP, Block BA. 2010 Philopatry and migration of Pacific white sharks. *Proceedings of the Royal Society B: Biological Sciences* **277**, 679–688.
40. Macdonald C, Perni N, Jerome J, Wester J, Black K, Shiffman D. 2021 First identification of probable nursery habitat for critically endangered great hammerhead Sphyrna mokarran on the Atlantic Coast of the United States. *Conservation Science and Practice* **3**, 1–6.
41. Cappetta H. 2012 *Handbook of Paleoichthyology, Volume 3E*. Munich: Verlag chondricht edition.
42. Cunningham SB. 2000 A comparison of isolated teeth of early Eocene Striatolamia macrota (Chondrichthyes , Lamniformes), with those of a Recent sand shark , Carcharias taurus. *Tertiary Research* **20**, 17–31.
43. Haulsee DE, Fox DA, Breece MW, Clauss TM, Oliver MJ. 2016 Implantation and recovery of long-term archival transceivers in a migratory shark with high site fidelity. *PloS one* **11**, e0148617.

44. Haulsee D, Breece M, Brown L, Wetherbee B, Fox D, Oliver M. 2018 Spatial ecology of Carcharias taurus in the northwestern Mid-Atlantic coastal ocean. *Marine Ecology Progress Series* **597**, 191–206.
45. Teter SM, Wetherbee BM, Fox DA, Lam CH, Kiefer DA, Shivji M. 2015 Migratory patterns and habitat use of the sand tiger shark (Carcharias taurus) in the western North Atlantic. *Marine and Freshwater Research* **66**, 158–169.
46. Kilfoil JP, Wetherbee BM, Carlson JK, Fox DA. 2017 Targeted catch-and-release of prohibited sharks: sand tigers in coastal Delaware waters. *Fisheries* **42**, 281–287.
47. Kneebone J, Chisholm J, Skomal GB. 2012 Seasonal residency, habitat use, and site fidelity of juvenile sand tiger sharks Carcharias taurus in a Massachusetts estuary. *Marine Ecology Progress Series* **471**, 165–181.
48. Goldman KJ, Branstetter S, Musick JA. 2006 A re-examination of the age and growth of sand tiger sharks, Carcharias taurus, in the western North Atlantic: The importance of ageing protocols and use of multiple back-calculation techniques. *Environmental Biology of Fishes* **77**, 241–252.
49. Cortés E, Parsons GR. 1996 Comparative demography of two populations of the bonnethead shark (Sphyrna tiburo). *Canadian Journal of Fisheries and Aquatic Sciences* **53**, 709–718.
50. Moses ME, Hou C, Woodruff WH, West GB, Nekola JC, Zuo W, Brown JH. 2008 Revisiting a Model of Ontogenetic Growth: Estimating Model Parameters from Theory and Data. *http://dx.doi.org.proxy.lib.sfu.ca/10.1086/679735* **171**, 632–645.
51. Gillooly JF, Charnov EL, West GB, Savage VM, Brown JH. 2002 Effects of size and temperature on developmental time. *Nature* **417**, 70–73.
52. Hou C, Zuo W, Moses ME, Woodruff WH, Brown JH, West GB. 2008 Energy Uptake and Allocation During Ontogeny. *Science* **322**, 736–739.
53. Kempes CP, Dutkiewicz S, Follows MJ. 2012 Growth, metabolic partitioning, and the size of microorganisms.. *PNAS* **109**, 495–500.
54. Pirt S. 1965 The maintenance energy of bacteria in growing cultures. *Proc. Roy. Soc. B* **163**, 224.
55. Heijnen JJ, Roels JA. 1981 A macroscopic model describing yield and maintenance relationships in aerobic fermentation processes. *Biotechnology and Bioengineering* **23**, 739–763.
56. Yeakel JD, Kempes CP, Redner S. 2018 Dynamics of starvation and recovery predict extinction risk and both Damuth's law and Cope's rule. *Nature communications* **9**, 1–10.
57. Brown JH, Gillooly JF, Allen AP, Savage VM, West GB. 2004 Toward a metabolic theory of ecology. *Ecology* **85**, 1771–1789.
58. Zeichner S, Colman A, Koch P, Polo-Silva C, Galván-Magaña F, Kim S. 2017 Discrimination factors and incorporation rates for organic matrix in shark teeth based on a captive feeding study. *Physiological and Biochemical Zoology* **90**, 257–272.
59. Cantrill DJ, Poole I. 2012 *The vegetation of Antarctica through geological time*. Cambridge University Press.
60. Miall AD. 1986 The Eureka Sound Group (Upper Cretaceous-Oligocene), Canadian Arctic Islands. *Bulletin of Canadian Petroleum Geology* **34**, 240–270.
61. Eberle JJ, Greenwood DR. 2012 Life at the top of the greenhouse Eocene world—A review of the Eocene flora and vertebrate fauna from Canada's High Arctic. *Bulletin* **124**, 3–23.
62. Marenssi SA, Net LI, Santillana SN. 2002 Provenance, environmental and paleogeographic controls on sandstone composition in an incised-valley system: the Eocene La Meseta Formation, Seymour Island, Antarctica. *Sedimentary Geology* **150**, 301–321.
63. Beard KC. 2008 The oldest North American primate and mammalian biogeography during the Paleocene–Eocene Thermal Maximum. *Proceedings of the National Academy of Sciences* **105**, 3815–3818.
64. Flis JE, Yancey TE, Flis CJ. 2017 Middle Eocene Storm Deposition in the Northwestern Gulf of Mexico, Burleson County, Texas, U.S.A. *Gulf Coast Association of Geological Societies* **6**, 201–225.
65. Heupel MR, Knip DM, Simpfendorfer CA, Dulvy NK. 2014 Sizing up the ecological role of sharks as predators. *Marine Ecology Progress Series* **495**, 291–298.
66. Kneebone J, Chisholm J, Skomal G. 2014 Movement patterns of juvenile sand tigers (Carcharias taurus) along the east coast of the USA. *Marine Biology* **161**, 1149–1163.

67. Otway N, Ellis M. 2011 Pop-up archival satellite tagging of Carcharias taurus: movements and depth/temperature-related use of south-eastern Australian waters. *Marine and Freshwater Research* **62**, 607–620.
68. Sluijs A, Röhl U, Schouten S, Brumsack HJ, Sangiorgi F, Damsté JSS, Brinkhuis H. 2008 Arctic late Paleocene–early Eocene paleoenvironments with special emphasis on the Paleocene-Eocene thermal maximum (Lomonosov Ridge, Integrated Ocean Drilling Program Expedition 302). *Paleoceanography* **23**.
69. Eberle JJ, Fricke HC, Humphrey JD, Hackett L, Newbrey MG, Hutchison JH. 2010 Seasonal variability in Arctic temperatures during early Eocene time. *Earth and Planetary Science Letters* **296**, 481–486.
70. West CK, Greenwood DR, Basinger JF. 2015 Was the Arctic Eocene 'rainforest'monsoonal? Estimates of seasonal precipitation from early Eocene megafloras from Ellesmere Island, Nunavut. *Earth and Planetary Science Letters* **427**, 18–30.
71. West CK, Greenwood DR, Reichgelt T, Lowe AJ, Vachon JM, Basinger JF. 2020 Paleobotanical proxies for early Eocene climates and ecosystems in northern North America from middle to high latitudes. *Climate of the Past* **16**, 1387–1410.
72. Zhu J, Poulsen CJ, Otto-Bliesner BL, Liu Z, Brady EC, Noone DC. 2020 Simulation of early Eocene water isotopes using an Earth system model and its implication for past climate reconstruction. *Earth and Planetary Science Letters* **537**, 116164.
73. Keating-Bitonti CR, Ivany LC, Affek HP, Douglas P, Samson SD. 2011 Warm, not super-hot, temperatures in the early Eocene subtropics. *Geology* **39**, 771–774.
74. Ivany LC, Wilkinson BH, Lohmann KC, Johnson ER, McElroy BJ, Cohen GJ. 2004 Intra-annual isotopic variation in Venericardia bivalves: implications for early Eocene temperature, seasonality, and salinity on the US Gulf Coast. *Journal of Sedimentary Research* **74**, 7–19.
75. Hopkins W. 1974 Report on 36 Field Samples from Banks Island, District of Franklin, Northwest Territories, Submitted by A. Miall, 1973 (NTS 88C, F, 98D, E), Geological Survey of Canada. Technical report Paleontological Report KT-01-WSH-1974.
76. Hopkins W. 1975 Palynology Report on 44 Field Samples from Banks Island, Submitted by AD Miall, 1974 (NTS 88B, C, F, 97H, 98D, E); Geological Survey of Canada. Technical report Paleontological Report KT-10-WSH-1975.
77. Miall AD. 1979 Mesozoic and Tertiary geology of Banks Island, Arctic Canada: the history of an unstable craton margin. *Geological Survey of Canada Memoir* **387**, 1–235.
78. Sweet A. 2012 Applied research report on 5 outcrop samples collected by Andrew Miall from northern Banks Island. *NWT (NTS Map Sheets 098E/01, 08, 09): Geological Survey of Canada Paleontological report ARS-2012-01*.
79. Eberle JJ, Gottfried MD, Hutchison JH, Brochu CA. 2014 First record of Eocene bony fishes and crocodyliforms from Canada's Western Arctic. *PloS one* **9**, e96079.
80. Stilwell JD, Zinsmeister WJ. 1992 *Molluscan systematics and biostratigraphy: Lower Tertiary La Meseta Formation, Seymour Island, Antarctic Peninsula*. Washington: American Geophysical Union antarctic edition.
81. Marenssi SA, Reguero MA, Santillana SN, Vizcaino SF. 1994 Review Eocene land mammals from Seymour Island, Antarctica: palaeobiogeographical implications. .
82. Amenábar CR, Montes M, Nozal F, Santillana S. 2020 Dinoflagellate cysts of the la Meseta Formation (middle to late Eocene), Antarctic Peninsula: Implications for biostratigraphy, palaeoceanography and palaeoenvironment. *Geological Magazine* **157**, 351–366.
83. Douglas PM, Affek HP, Ivany LC, Houben AJ, Sijp WP, Sluijs A, Schouten S, Pagani M. 2014 Pronounced zonal heterogeneity in Eocene southern high-latitude sea surface temperatures. *Proceedings of the National Academy of Sciences* **111**, 6582–6587.
84. Eagles G, Livermore R, Morris P. 2006 Small basins in the Scotia Sea: the Eocene Drake passage gateway. *Earth and Planetary Science Letters* **242**, 343–353.
85. Scher HD, Martin EE. 2006 Timing and climatic consequences of the opening of Drake Passage. *science* **312**, 428–430.
86. Harrington GJ. 2003 Wasatchian (Early Eocene) pollen floras from the Red Hot Truck Stop, Mississippi, USA. *Palaeontology* **46**, 725–738.

87. Basinger J, Greenwood D, Sweda T. 1994 Early Tertiary vegetation of Arctic Canada and its relevance to paleoclimatic interpretation. In *Cenozoic plants and climates of the Arctic* , pp. 175–198. Springer.
88. Sluijs A, Schouten S, Donders TH, Schoon PL, Röhl U, Reichart GJ, Sangiorgi F, Kim JH, Damsté JSS, Brinkhuis H. 2009 Warm and wet conditions in the Arctic region during Eocene Thermal Maximum 2. *Nature Geoscience* **2**, 777–780.
89. Kobashi T, Grossman EL. 2003 The oxygen isotopic record of seasonality in Conus shells and its application to understanding late middle Eocene (38 Ma) climate. *Paleontological Research* **7**, 343–355.
90. Montes M, Beamud E, Nozal F, Santillana S. 2019 Late Maastrichtian-Paleocene chronostratigraphy from Seymour Island (James Ross Basin, Antarctic Peninsula). Eustatic controls of sedimentation. *Advances in Polar Science* **30**, 303–327.
91. Jorgensen SJ, Arnoldi NS, Estess EE, Chapple TK, Rückert M, Anderson SD, Block BA. 2012 Eating or meeting? Cluster analysis reveals intricacies of white shark (Carcharodon carcharias) migration and offshore behavior. *PloS one* **7**, e47819.
92. Dicken ML, Booth AJ, Smale MJ. 2008 Estimates of juvenile and adult raggedtooth shark (Carcharias taurus) abundance along the east coast of South Africa. *Canadian Journal of Fisheries and Aquatic Sciences* **65**, 621–632.
93. Castro JI. 1987 The position of sharks in marine biological communities: an overview. *Sharks, An Inquiry into Biology, Behavior, Fisheries, and Use* pp. 11–17.
94. Kinney MJ, Simpfendorfer CA. 2009 Reassessing the value of nursery areas to shark conservation and management. *Conservation letters* **2**, 53–60.
95. McClain CR, Balk MA, Benfield MC, Branch TA, Chen C, Cosgrove J, Dove AD, Gaskins L, Helm RR, Hochberg FG et al.. 2015 Sizing ocean giants: patterns of intraspecific size variation in marine megafauna. *PeerJ* **3**, e715.
96. Watanabe YY, Papastamatiou YP. 2019 Distribution, body size and biology of the megamouth shark Megachasma pelagios. *Journal of fish biology* **95**, 992–998.
97. Pimiento C, Balk MA. 2015 Body-size trends of the extinct giant shark Carcharocles megalodon: a deep-time perspective on marine apex predators. *Paleobiology* **41**, 479–490.
98. Shimada K. 2005 Types of tooth sets in the fossil record of sharks, and comments on reconstructing dentitions of extinct sharks. *Journal of Fossil Research* **38**, 141–145.
99. Whitenack LB, Kim SL, Sibert EC. in press Bridging the Gap Between Chondrichthyan Paleobiology and Biology. *Biology of sharks and their relatives* **3**.